

## ADCs Dynamic Testing by Multiharmonic Sine Fitting Algorithms

Dominique Dallet<sup>1</sup>, Dario Petri<sup>2</sup>, Daniel Belega<sup>3</sup>

<sup>1</sup> *IMS Laboratory, University of Bordeaux- IPB ENSEIRB MATMECA*

*351 Cours de la Libération, Bâtiment A31, 33405, Talence Cedex, France,*

*Phone : +33 5 40 00 26 32, Fax : +33 5 56 37 15 45, E-mail: dominique.dallet@ims-bordeaux.fr*

<sup>2</sup> *Department of Ingegneria e Scienza dell'Informazione, University of Trento,*

*Via Sommarive, 14-38100, Trento, Italy,*

*Phone : +39 0461 883902, Fax : +39 0461 882093, E-mail: petri@disi.unitn.it*

<sup>3</sup> *Faculty of Electronics and Telecommunications, "Politehnica" University of Timișoara,*

*Bv. V. Pârvan, Nr. 2, 300223, Timisoara, Romania,*

*Phone : +40 2 56 40 33 65, Fax : +40 2 56 40 33 62, E-mail: daniel.belega@etc.upt.ro*

**Abstract-** The paper investigates and compares the performances of two state-of-the-art MultiHarmonic Sine Fitting (MHSF) algorithms when used in the dynamic testing of an Analog-to-Digital Converter (ADC). The influence of the initial estimate of the test signal frequency on the uncertainty of the estimated ADC dynamic parameters is analyzed by using computer simulations. Moreover, the accuracies of the considered MHSF algorithms and the sine-fit algorithms suggested in the existing standards for ADCs testing are compared by means of both computer simulations and experimental results.

### I. Introduction

The three-parameter sine-fit (3PSF) and four-parameter sine-fit (4PSF) algorithms are widely used in the estimation of the parameters of a sine-wave [1] – [6]. Indeed, they are robust with respect to the non-coherent sampling, provide accurate estimates, and are simple to implement. Due to the good features of these algorithms, both the IEEE Standard 1241 for Analog-to-Digital Converters (ADCs) [1] and the European Project DYNAD for dynamic testing of ADCs [2] suggest their use for the estimation of ADC dynamic parameters such as the Signal-to-Noise And Distortion (*SINAD*) ratio and the Effective Number Of Bits (*ENOB*). Unfortunately, when considering a harmonically distorted sine-wave, the 3PSF and 4PSF algorithms do not allow the estimation of some important parameters such as the Total Harmonic Distortion (*THD*), the Spurious Free Dynamic Range (*SFDR*), and the Signal-Noise and Harmonic Ratio (*SNHR*). To overcome this problem MultiHarmonic Sine Fitting (MHSF) algorithms have been proposed [7], [8]. However, the performance of MHSF algorithms when applied in the ADC dynamic testing has not been yet analyzed in the scientific literature.

The aim of this paper is to analyse the accuracy achieved in ADC dynamic testing when applying the MHSF algorithm proposed in [7] (denoted as the MHSF1) and the MHSF algorithms presented in [8] (denoted as MHSF2a and MHSF2b, when the signal frequency is respectively known or unknown). Specifically, the effect of the accuracy of the initial value of the signal frequency on the uncertainty of the estimated ADC dynamic parameters is investigated. Moreover, the *ENOB* estimation accuracies provided by the considered MHSF algorithms and the 3PSF and 4PSF algorithms are compared by means of both computer simulations and experimental results. In addition, the accuracies of the harmonic amplitudes of an ADC output signal achieved by the considered MHSF algorithms are compared through computer simulations and experimental results.

### II. Influence of the accuracy of the initial value of the test signal normalized frequency

Let us consider an ADC fed by a pure sine-wave. The ADC output signal can be expressed as:

$$y(m) = A \sin\left(2\pi \frac{f_{in}}{f_s} m + \varphi\right) + d + r(m), \quad m = 0, 1, 2, \dots \quad (1)$$

where  $A$ ,  $f_{in}$ ,  $\varphi$ , and  $d$  are respectively the amplitude, the frequency, the phase and the offset of the output sine-wave,  $f_s$  is the ADC sampling frequency, and  $r(\cdot)$  is the ADC output noise. The noise  $r(\cdot)$  represents the overall error introduced by the converter and includes the effects of random noise, fixed pattern errors, nonlinearities (e.g. harmonic or spurious components), aperture uncertainty, etc.

When  $M$  samples are acquired, the ratio between the frequencies  $f_{in}$  and  $f_s$ , can be expressed as:

$$\frac{f_{in}}{f_s} = \frac{\lambda_0}{M} = \frac{l + \delta}{M}, \quad (2)$$

where  $l$  and  $\delta$  ( $-0.5 \leq \delta < 0.5$ ) are respectively the integer and the fractional parts of the number of acquired sine-wave cycles  $\lambda_0$ . The frequency  $f_{in}$  is chosen smaller than  $f_s/2$  to satisfy the Nyquist theorem. Notice that the parameter  $\lambda_0$  represents also the sine-wave normalized frequency expressed in bins and it is usually evaluated by estimating  $l$  and  $\delta$  separately. It is worth noticing that coherent sampling imply  $\delta = 0$ , but a non-coherent sampling (that is  $\delta \neq 0$ ) is very common in practical applications.

The analysis was performed by means of computers simulations in which the ADC output signal was synthesized as a sine-wave, its second, third, fourth harmonics, and noise. The second harmonic amplitude was set to  $4Q/\sqrt{21}$ , where  $Q$  is the theoretical code bin width of an  $n$ -bit ADC with Full Scale-Range ( $FSR$ ) equal to 10. The third and the fourth harmonic amplitudes were respectively two- and four-times smaller than the second harmonic one. The noise was synthesized as the summation of both quantization and Gaussian noise and its power was determined by assuming a theoretical  $ENOB$  equal to  $(n - 1.5)$  bits. The integer and fractional parts  $l$  and  $\delta$  of the number of acquired sine-wave cycles were set to 73 and  $-0.5$ , respectively. This value of  $\delta$  was chosen since it maximizes the contribution of the spectral interference due to the image component on the normalized frequency estimate [9]. The record length was set to  $M = 1024$ , the sampling frequency was  $f_s = 1$  MHz, while the ADC resolution  $n$ , was varied in the range [8, 24] bits with a step of 2 bits. The predefined threshold on the estimated frequency changes used in the iteration stopping condition of the MHSF algorithms was equal to  $10^{-6}$ . The Interpolated Discrete Fourier Transform (IpDFT) method based on the  $H$ -term maximum sidelobe decay windows ( $H \geq 1$ ) was used for estimating the initial value of the sine-wave frequency. For each value of  $n$ , 1000 runs were performed by varying at random the initial phases of the fundamental and harmonic components. Then, the  $ENOB$  estimates provided by the MHSF algorithms were determined.

Fig. 1 shows the magnitude of the bias of  $ENOB$  estimates achieved by the MHSF1 (Fig.1 (a)) and MHSF2b (Fig. 1(b)) algorithms as a function of the theoretical  $ENOB$ . The initial value of the sine-wave frequency was estimated by the IpDFT method based on the two- ( $H = 2$ ) and three-term ( $H = 3$ ) maximum sidelobe decay windows when using the MHSF1 algorithm. Conversely, the rectangular ( $H = 1$ ) and two-term ( $H = 2$ ) maximum sidelobe decay windows were adopted when the MHSF2b algorithm was employed. It should be noticed that only the rectangular window was considered in [8].

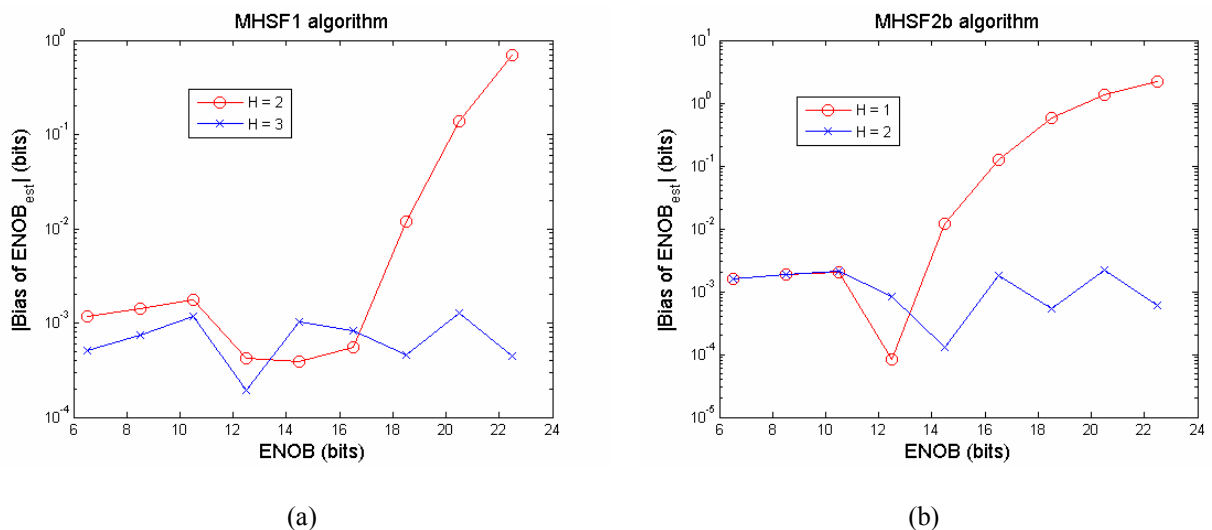


Figure 1. Magnitude of the  $ENOB$  estimation bias achieved by the MHSF1 (a) and MHSF2b (b) algorithms versus the theoretical  $ENOB$ . The initial value of the sine-wave normalized frequency was estimated by the IpDFT method based on the rectangular ( $H = 1$ ), two-term ( $H = 2$ ) and three-term ( $H = 3$ ) maximum sidelobe decay windows.

Fig. 1(a) shows that the  $ENOB$  parameter is accurately estimated by the MHSF1 algorithm up to a theoretical  $ENOB$  of 18.5 bits when the two-term sidelobe decay window is used and for all the considered ADC resolutions when the three-term maximum sidelobe decay window is adopted. Differently, the estimated  $ENOB$  is accurate only up to  $ENOB = 6.5$  bits if the rectangular window is used.

When the MHSF2b algorithm is employed the  $ENOB$  parameter is estimated with high accuracy up to  $ENOB = 14.5$  bits when the rectangular window is adopted and for all the considered ADC resolutions if the two-term maximum sidelobe decay window is used.

Thus we can conclude that the MHSF2b algorithm is more robust than the MHSF1 algorithm to inaccuracies in the initial value of the sine-wave frequency. Moreover, simulations results showed that, if the initial estimate of the sine-wave frequency was achieved by the IpDFT method based on the two-term maximum sidelobe decay window, the  $ENOB$  of an ADC with resolution up to 24 bits can be accurately estimated by the MHSF2b algorithm as soon as  $l \geq 8$  and by the MHSF1 algorithm when  $l \geq 201$ . In addition, if the initial value of the sine-wave frequency is provided by the IpDFT method based on the three-term maximum sidelobe decay window, the  $ENOB$  can be estimated with high accuracy by the MHSF1 algorithm if  $l \geq 43$ .

### III. Accuracy performance of the MHSF1, MHSF2a, and MHSF2b algorithms

The aim of this section is to compare the accuracy performance of the MHSF algorithms and the 3PSF and 4PSF algorithms when estimating the  $ENOB$  of an ADC. The performance of the MHSF algorithms when estimating the amplitudes of the ADC output harmonic components are also analysed. All reported results were achieved through computer simulations.

#### A. $ENOB$ estimation

The harmonic components of a real ADC output signal are much smaller than the fundamental component. Therefore, the initial estimate of the sine-wave frequency required by the MHSF2a and the 3PSF algorithms can be achieved by using the IpDFT method based on the  $H$ -term maximum sidelobe decay window ( $H \geq 2$ ) [10]. Moreover, the optimal window to be adopted can be determined according to the criterion proposed in [11].

The same simulation parameters used in the previous section were considered. Fig. 2 shows the magnitude of the bias and the standard deviation of the  $ENOB$  estimates provided by the MHSF1, MHSF2a, MHSF2b, 3PSF, and 4PSF algorithms as a function of the theoretical  $ENOB$ . In the MHSF1 and MHSF2b algorithms the three-term and two-term maximum sidelobe decay windows were adopted, respectively. According to the criterion proposed in [11], in the MHSF2a and 3PSF algorithms the three-term maximum sidelobe decay window was used. In the 4PSF algorithm the initial sine-wave parameters were estimated by the IpDFT method based on the rectangular window [6]. The iteration stopping condition required that the magnitude of the difference between two consecutive estimates was smaller than  $10^{-6}$  for each parameter.

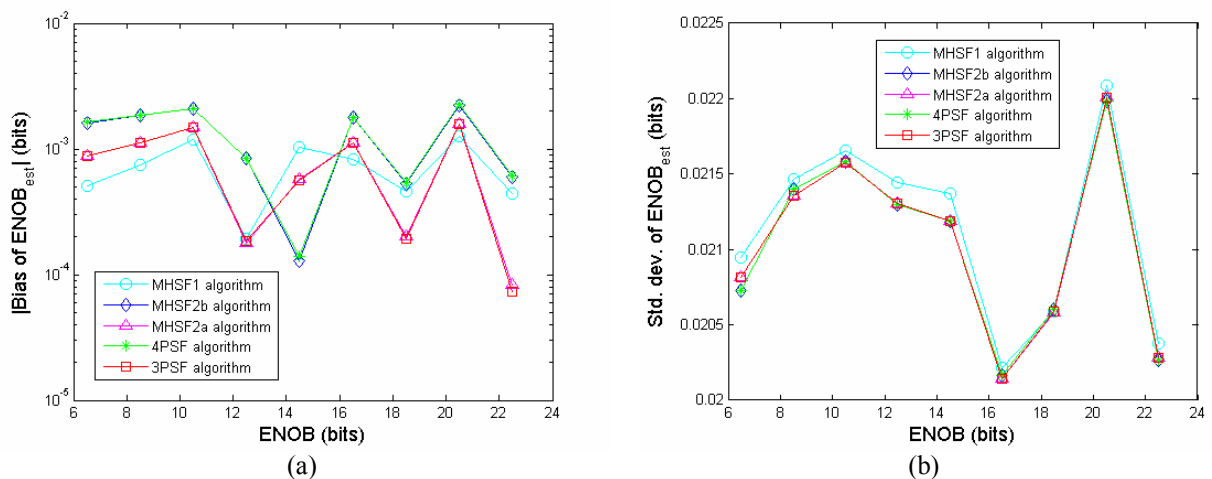


Figure 2. Magnitude of the  $ENOB$  bias (a) and standard deviation (b) for the MHSF1, MHSF2a, MHSF2b, 3PSF, and 4PSF algorithms versus the theoretical  $ENOB$ .

Fig. 1 shows that all the considered algorithms are very accurate and provide results close each other. Moreover, the results achieved by the MHSF2b and the 4PSF algorithms are almost identical. The same conclusion holds for the MHSF2a and the 3PSF algorithms.

It should be noticed that the same behaviour occurs when estimating the  $SINAD$  parameter. Indeed a linear relationship exists between  $ENOB$  and  $SINAD$  parameters.

## B. Estimation the amplitudes of the ADC output harmonic components

To achieve high accuracy estimates of the  $THD$  and  $SNHR$  parameters, usually we need accurate estimates of the amplitudes of the harmonic components of the ADC output signal. Thus, the estimation uncertainty of the amplitudes of the ADC output harmonic components is investigated in the following.

In Fig. 3 the magnitude of the estimation bias achieved by the considered MHSF algorithms on the amplitudes of the 2<sup>nd</sup> and 4<sup>th</sup> harmonic components is depicted as a function of the theoretical  $ENOB$ . The statistical efficiency of the amplitude estimator provided by each MHSF algorithm with respect to the related single-tone unbiased Cramér-Rao Lower Bound (CRLB) [12] is also depicted for the same harmonic components.

Simulation results shows that all the considered MHSF algorithms estimate the 2<sup>nd</sup> and 4<sup>th</sup> harmonic component amplitudes with very similar and very high accuracy. Moreover, the statistical efficiencies of the achieved estimators are very close to 1. The same behaviour was achieved in the estimation of the amplitudes of the fundamental and of the 3<sup>rd</sup> harmonic components. Other simulations with different values of  $FSR$ ,  $l$ ,  $\delta$ , and Gaussian noise power were performed. The same behaviour as in Figs. 2 and 3 was always achieved.

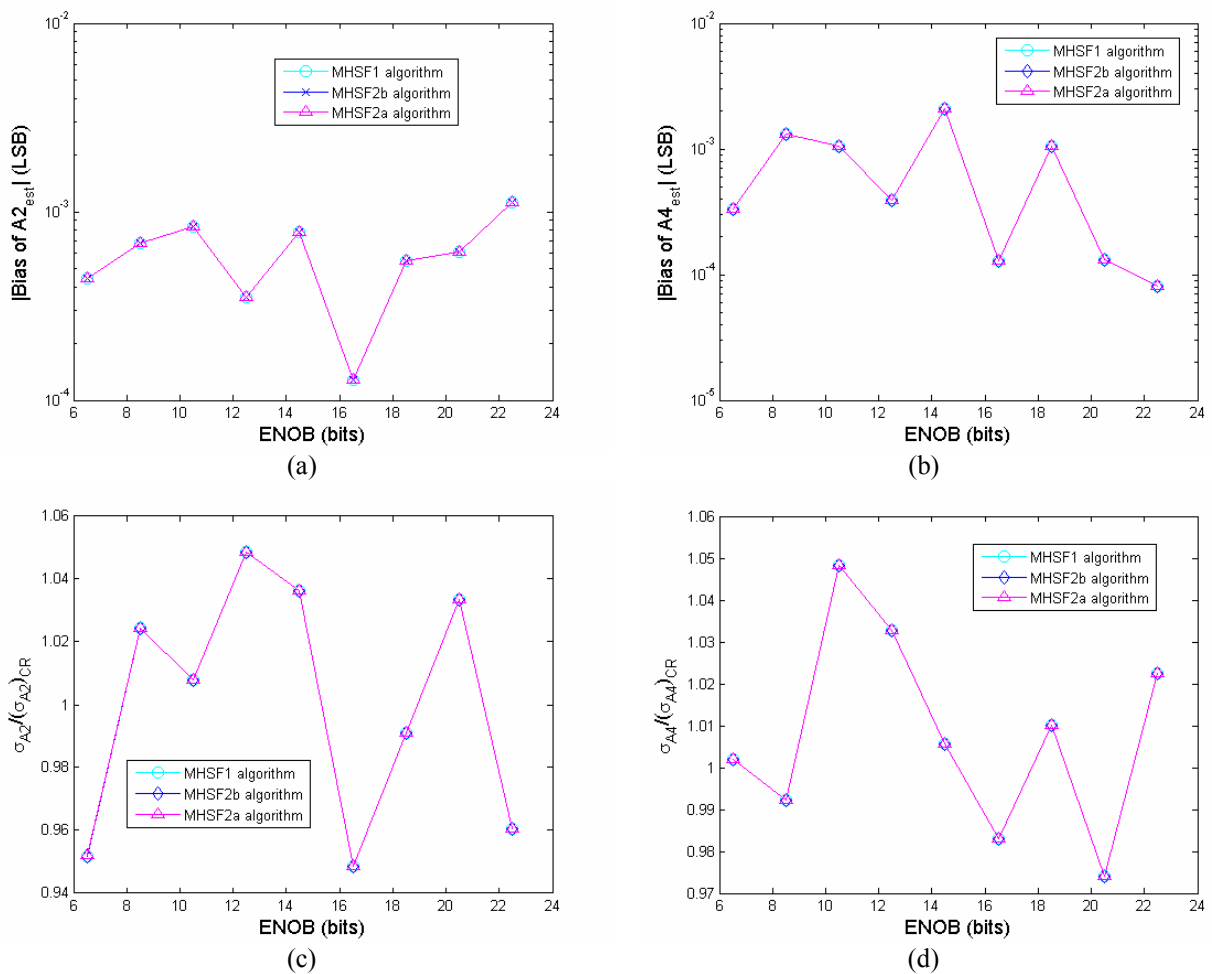


Figure 3. Magnitude of the bias (a), (b) and statistical efficiency (c), (d) of the amplitude estimates of 2<sup>nd</sup> and 4<sup>th</sup> harmonic components of the ADC output signal provided by the MHSF1, MHSF2a, and MHSF2b algorithms versus the theoretical  $ENOB$ .

Finally, the processing times required by the MHSF1, MHSF2a, and MHSF2b algorithms were compared when considering an ADC resolution of 16 bits. The algorithms were implemented in MATLAB 7.0 running on a portable computer with a processor clock of 2 GHz. The average processing time required by each algorithm over 1000 records were 428.47, 25.78, 51.87 ms for the MHSF1, MHSF2a, and MHSF2b algorithms, respectively. Thus, the MHSF2a and MHSF2b algorithms exhibits a much better processing efficiency than the MHSF algorithm.

#### IV. Experimental results

The considered MHSF, 3PSF and 4PSF algorithms were applied to data acquired by a 12-bit data acquisition board NI-6023E, developed by the National Instruments. The *FSR* and the sampling frequency were set to 10 V and 100 kHz, respectively. The test sine-waves were supplied by an Agilent 33220A signal generator and characterized by an amplitude of 5 V and frequencies 3.1, 7.9, 12.3, 17.5, 22.1, and 26.7 kHz, respectively. For each value of frequency, 1000 records of  $M = 1024$  samples each were acquired. Then the *ENOB* parameter and the amplitudes of the fundamental and the harmonic components up to the 5<sup>th</sup> order were estimated. The initial value for the sine-wave normalized frequency was estimated by using the IpDFT method based on the three-term or the two-term maximum sidelobe decay window respectively when the MHSF1 algorithm or the MHSF2a, MHSF2b, and 3PSF algorithms were employed. Fig. 4 shows the mean and the standard deviation of the *ENOB* estimates achieved by the considered algorithms as a function of the test sine-wave frequency. It should be noticed that we considered the mean value instead of the bias since the true value of the *ENOB* is unknown. However, this is irrelevant when comparing the algorithm accuracies since differences between mean values or between biases coincides.

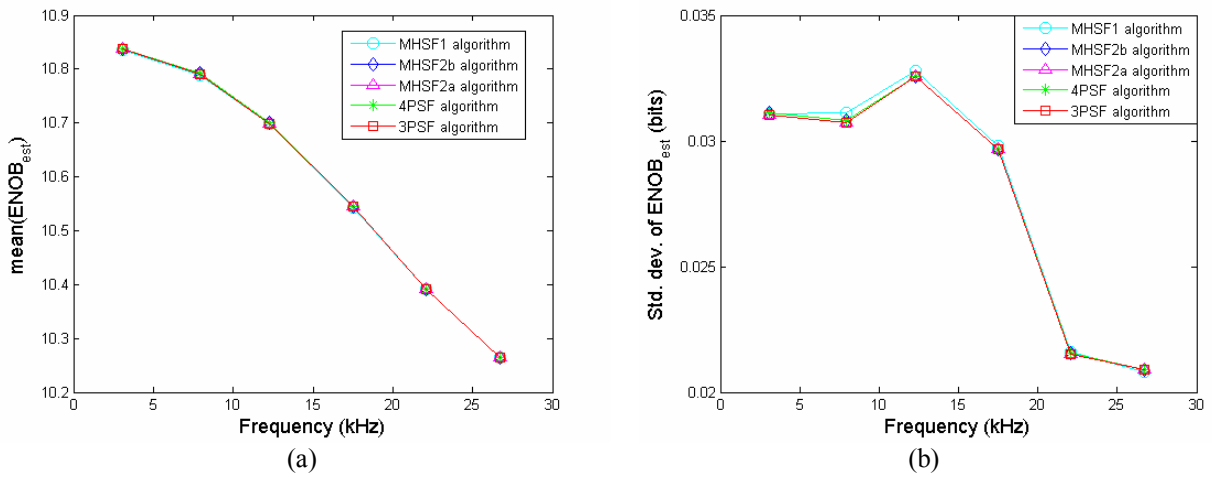


Figure 4. Mean (a) and standard deviation (b) of the *ENOB* estimates achieved by the MHSF1, MHSF2a, MHSF2b, 3PSF, and 4PSF algorithms versus the test sine-wave frequency.

Experimental results show that the mean and the standard deviation of the *ENOB* estimates achieved by the considered methods are almost equal. In particular, the magnitude of the difference between the mean values of the *ENOB* estimates provided by the MHSF2a and 3PSF algorithms is about  $6.4 \cdot 10^{-6}$  bits, while it is equal to  $8.7 \cdot 10^{-6}$  bits for the MHSF2b and 4PSF algorithms.

The mean and the standard deviation of the amplitude of the fundamental and the harmonic components estimated by the MHSF1, MHSF2a, and MHSF2b algorithms at the 26.7 kHz are given in Table I. As already occurred with simulations, the experimental results provided by all the algorithms are very close each other. The same happened for other test sine-wave frequencies.

Table I. Mean and standard deviation of the amplitude estimates provided by the MHSF1, MHSF2a, and MHSF2b algorithms.

	MHSF1 algorithm		MHSF2a algorithm		MHSF2b algorithm	
	mean [LSB]	std. dev. [LSB]	mean [LSB]	std. dev. [LSB]	mean [LSB]	std. dev. [LSB]
fundamental	2040.07608	2.94700E-2	2040.07608	2.94697E-2	2040.07608	2.94705E-2
2nd harmonic	4.49576E-1	2.98081E-2	4.49578E-1	2.98083E-2	4.49579E-1	2.98082E-2
3rd harmonic	9.16448E-1	1.71615E-2	9.16444E-1	1.71597E-2	9.16446E-1	1.71612E-2
4th harmonic	5.25190E-2	1.42841E-2	5.25186E-2	1.42834E-2	5.25175E-2	1.42850E-2
5th harmonic	6.44283E-2	1.49024E-2	6.44310E-2	1.49015E-2	6.44290E-2	1.49012E-2

## V. Conclusions

The paper dealt with the application of the MSHF1, MSHF2a, and MSHF2b algorithms to the dynamic testing of ADCs. It has been shown that the robustness of the MSHF2b algorithm to inaccuracies in the initial value of the sine-wave frequency is higher than of the MSHF1 algorithm. To estimate the *SINAD* and *ENOB* parameters the initial value of the sine-wave frequency can be estimated by the lpDFT method based on the three-term or the two-term maximum sidelobe decay window when the MSHF1 algorithm or the MSHF2b algorithm is employed, respectively. Also, when estimating *SINAD* and *ENOB* parameters, all the considered MSHF algorithms provide the same estimation accuracy as the well-known 3PSF and 4PSF algorithms.

In addition, the MSHF algorithms allow to achieve very accurate *THD* and *SNHR* estimates. In particular, they exhibit the same accuracy when estimating the amplitudes of the ADC output harmonic components. However, the MSHF2a and MSHF2b algorithms are quite faster and are easier to implement than the MSHF1 algorithm. Also, the MSHF1 algorithm can be hardly applied when the number of the acquired samples is high.

For these reasons the authors believe that the MSHF2a and MSHF2b algorithms could be advantageously included in the existing standards for ADCs dynamic testing.

## References

- [1] IEEE Std. 1241, Standard for Terminology and Test Methods for Analog-to-Digital Converters, Tech. rep. IEEE-TC10, December, 2000.
- [2] European Project DYNAD. Methods and Draft Standards for the Dynamic Characterization and Testing of Analog-to-Digital Converters.
- [3] P. Händel, "Properties of the IEEE-STD-1057 four-parameter sine wave fit algorithm," *IEEE Trans. Instrum. Meas.*, vol. 49, no. 6, pp. 1189-1193, December 2000.
- [4] T. Andersson and P. Händel, "IEEE standard 1057, Cramér-Rao bound and the parsimony principle," *IEEE Trans. Instrum. Meas.*, vol. 55, no. 1, pp. 44-53, February 2006.
- [5] D. Belega and D. Dallet, "Normalized frequency estimation for accurate dynamic characterization of A/D converters by means of the three-parameter sine-fit algorithm," *Measurement*, vol. 41, no. 9, pp. 986-993, November 2008.
- [6] T. Z. Bilau, T. Megyeri, A. Sárhegyi, J. Márkus, and I. Kollár, "Four-parameter fitting of sine wave testing result: iteration and convergence," *Comput. Stand. Interfaces*, vol. 26, no. 1, pp. 51-56, January 2004.
- [7] R. Pintelon and J. Schoukens, "An improved sine-wave fitting procedure for characterizing data acquisition channels," *IEEE Trans. Instrum. and Meas.*, vol. 45, no. 2, pp. 588-593, April 1996.
- [8] P. M. Ramos, M. F. da Silva, R. C. Martins, and A. M. Cruz Serra, "Simulation and experimental results of multiharmonic least-squares fitting algorithms applied to periodic signals," *IEEE Trans. Instrum. and Meas.*, vol. 55, no. 2, pp. 646-651, April 2006.
- [9] D. Belega and D. Dallet, "Choice of the acquisition parameters for frequency estimation of a sine wave by interpolated DFT method," *Computer, Standards & Interfaces*, vol. 31, no. 5, pp. 962-968, September 2009.
- [10] D. Belega and D. Dallet, "Evaluation of the dynamic performance of an A/D converter by means of the three-parameter sine-fit algorithm," IEEE International Mixed-Signals, Sensors, and Systems Test Workshop (IMSTW), pp. 1-6, Arizona, USA, 10-12 June, 2009.
- [11] D. Belega, D. Dallet, and D. Petri, "A high performance procedure for effective number of bits estimation in analog-to-digital converters," *IEEE Trans. Instrum. and Meas.*, vol. 60, no. 5, pp. 1522-1532, May 2011.
- [12] C. Offelli and D. Petri, "The influence of windowing on the accuracy of multifrequency signal parameter estimation," *IEEE Trans. Instrum. and Meas.*, vol. 41, no. 2, pp. 256-261, April 1992.